MAGNETIC SUSPENSION STABILITY OF THE NIST VACUUM-TO-AIR MASS DISSEMINATION SYSTEM

Corey Stambaugh*
Mass and Force Group, Quantum Measurement Division, NIST, U.S.A.

ABSTRACT

High precision mass comparisons are typically performed such that both masses are measured under nearly identical conditions. However, there are situations where an artifact needs to be calibrated against a standard kept under different conditions. For example, the new realization of the kilogram will be carried out in vacuum but the majority of calibrations services are performed at atmospheric pressure. At the National Institute of Standards and Technology we have developed an apparatus to perform direct mass comparison under such a condition using a magnetic suspension system. The stability of the magnetically suspended portion of the system plays a large role in the overall uncertainty of a measurement. Here we describe the control system for the magnetic suspension and the improvements we have made to increase its stability.

Keywords: Mass, magnetic suspension, kilogram, mise-en-pratique

1. INTRODUCTION

The redefinition of the kilogram will cut the tie to a physical artifact by using, for example, the watt balance to define the kilogram in terms of Planck's constant [1]. To realize this definition the magnitude of Planck's constant will be fixed. Overall, mass dissemination will remain the same after redefinition and mass comparators and artifacts will still be used. However, in the new definition the kilogram will be realized in vacuum; unlike the international prototype kilogram which is kept in air. Below the national metrology level, mass calibration will still be carried out in air. As such, a reliable method for accounting for mass changes, from sorption effects, when moving from vacuum-to-air, is required.

To date the primary method for vacuum-to-air transfer involves developing a model for the sorption effects. In this procedure the mass comparison is carried out in vacuum and then the test mass is brought to air. At that time an additional mass based on the sorption model would be added to the calibrated mass value. In this indirect way, mass calibration can be performed between vacuum and air.

At the National Institute of Standards and Technology (NIST) we are implementing a unique and direct alternative approach. Here the standard artifact is kept in vacuum while the test mass is kept in air. The mass comparison, performed using a single precision comparator, is carried out by coupling an upper assembly (mass comparator and mass pan in vacuum) to a lower assembly (mass pan in air) through magnetic suspension. Through this direct vacuum-to-air comparison the need to adjust measurements *post hoc* to account for mass changes resulting from sorption effects is eliminated.

To aid in characterizing and improving the overall performance of the magnetic suspension system in the NIST vacuum-to-air mass dissemination system a proof of concept (POC) system has been built. This testing bed has allowed us to focus on just the magnetic suspension system (MSS). The MSS can further be broken down into several key components: (1) the actuator, (2) the sensor, and (3) the control loop. In this paper we will focus on the control loop and its implementation using a field programmable gate array (FPGA).

2. PRINCIPLES

2.1 VACUUM-TO-AIR MASS DISEMINATION

*corresponding author information: C. Stambaugh corey.stambaugh@nist.gov; phone 1 301 975 3218; National Institute of Standards and Technology, Gaithersburg, MD 20899, U. S. A.

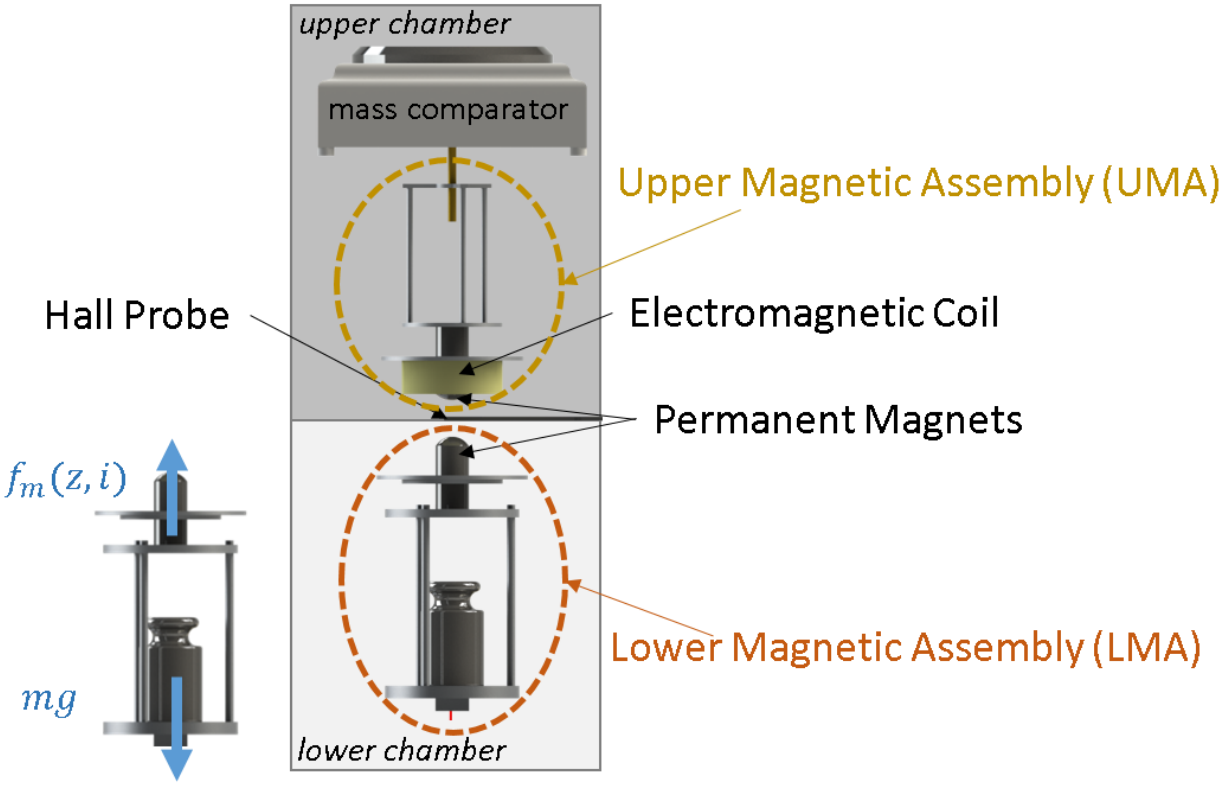

Figure 1: Illustration of essential components of proof of concept used for testing magnetic suspension. The POC is housed in a single box, here an upper and lower chamber is shown to illustrate how the system will be segregated in the actual system. The diagram on the lower left shows the main two forces acting on the suspended lower magnetic assembly (LMA).

Before delving deeply into the control system, a brief description of the operating principle for vacuum-to-air mass dissemination and for the magnetic suspension is warranted. For any standard mass comparison an unknown mass is compared to a known reference mass of nominally the same mass. In the case of mass comparators this is done by first weighing one of the two masses on a mass comparator. The result is recorded and then the other mass is weighed using the same comparator. The difference in the two readings is used to determine the actual mass of the unknown with respect to the known reference mass. Vacuum-to-air mass dissemination works the same, in principle, except one of the two masses is kept in vacuum while the other is kept in air.

As shown in Fig. 1, the mass comparator is placed in a vacuum chamber and the upper magnetic assembly (UMA) is hung from it. Below the vacuum chamber is a second chamber that will be kept in air. To couple the lower magnetic assembly (LMA) to the mass comparator in the vacuum chamber magnetic suspension is utilized. When the magnetic suspension is engaged the suspended LMA is coupled to the UMA and the mass comparator and thus its mass can effectively be removed from the measurement. The measurement sequence is now straightforward. Place the known mass on the UMA and ensure the LMA is suspended. Take a reading. Remove the mass from the UMA and turn off the suspension. Load the unknown mass on to the LMA and reengage the suspension. The difference between this reading and the prior one is the difference between the masses less corrections for air buoyancy and the gravitational difference resulting from the masses being placed at different heights.

2.2 MAGNETIC SUSPENSION

In the above measurement magnetic suspension plays the crucial role of coupling the suspended LMA to the UMA and subsequently the mass comparator. The basic principle behind the suspension is as follows. Attached to the lower and upper mass pans are two permanent magnets. These provide the majority of the necessary lifting force. Additionally, an

electromagnetic coil is wound around the upper magnet. A hall sensor is placed between the two permanent magnets and used to monitor the separation between the suspended LMA and the UMA. The hall sensor provides a proportional voltage which is fed to the control system. The control system outputs a voltage that provides the necessary current to the coil to counteract the motion of the suspended LMA in order to keep it suspended.

3. CONTROL SYSTEM

The implementation of a control loop to sustain suspension of the LMA is paramount to achieving stability in the mass readings. To aid in understanding the control system, we construct the closed-loop system as shown in Fig. 2. By calculating or measuring the values of the different components, a complete model can be developed. This model can then be simulated using tools like MATLAB Simulink[1]. Different parameters for the proportional-integrator-derivative (PID) controller can then be tested for stability. The results can be then be verified in the POC. The accurate realization of the POC in the model is vital for several reasons: (i) it provides a means to assess which parameters provide the most stable response, (2) it allows for an assessment of our knowledge of the magnetic suspension system, (3) it provides a convenient viewpoint to identify the major sources of instability, and (4) helps insure that when the final system is built we do not waste time determining the stable operation point. In this section, we describe each component in the closed-loop, state how their values were determined and compare the model's operation to actual suspension in the POC.

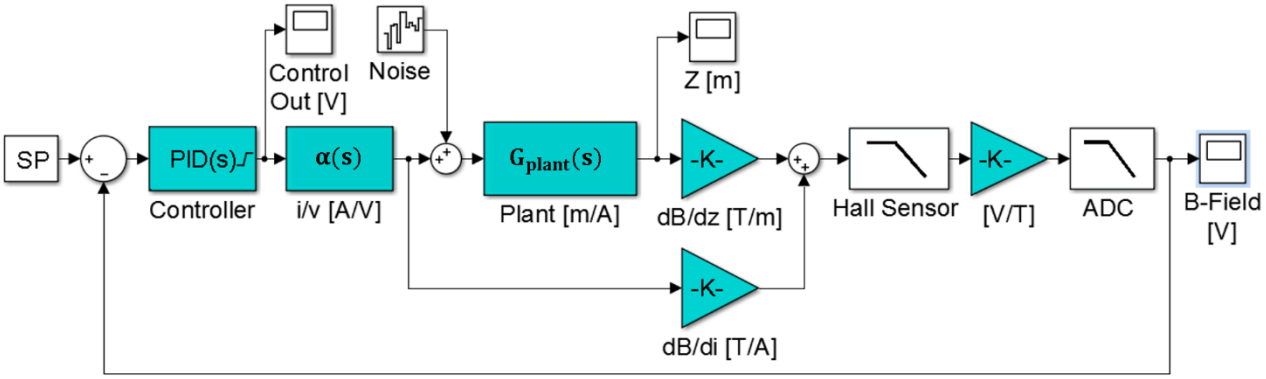

Figure 2: Schematic of the closed-loop control. SP, the setpoint, is chosen to be the magnetic field value (converted to voltage) measured by the probe when the relation $f_p(z_0) = mg$ holds. The PID controller is implemented on a FPGA chip to eliminate latency and time jitter.

3.1 CLOSED-LOOP

To the right of the controller block in Fig. 2 is the i/v block. This block converts the applied voltage to a current and consists of an amplifier and the electrical-side of the electromagnetic coil. The amplifier takes the controller output and amplifies by a gain A. For simplicity, we take the coil to be an RL filter. The resistance R is the resistance of the coil wire and the leads. The inductor L is the inductance of the coil. Their values are $R \approx 45\ \Omega$ and $L \approx 160$ mH. All together they form a low-pass filter with gain A, whose transfer function is

$$\alpha(s) = \frac{A}{L\,s + R}. \tag{1}$$

The RL filter has a cutoff frequency of ~45 Hz.

[1] Certain commercial equipment, instruments, or materials are identified in this paper in order to specify the experimental procedure adequately. Such identification is not intended to imply recommendation or endorsement by the National Institute of Standards and Technology, nor is it intended to imply that the materials or equipment identified are necessarily the best available for the purpose.

The current now works, as described by the plant, to produce a force that will act upon the LMA. The plant operation is determine by solving the equation of motion, assuming negligible damping, for the LMA, under the influence of gravity, g, and the magnetic field, $f_m(z,i)$:

$$m\ddot{z} = f_m(z,i) - mg. \tag{2}$$

Here $f_m(z,i)$ is the sum of the force generated by the permanent magnets f_p at a separation z and the force generated by the electromagnet with a current i and m is the total mass of the LMA (this can be with or without the test mass). For small motion Eq. 2 can be linearized by expanding $f_m(z,i)$:

$$m\ddot{z} = f_p(z_0) + k_z z(t) + k_i i(t) - mg. \tag{3}$$

The parameters k_z and k_i represent the force gradients with respect to z for the permanent magnet and i for the coil. By choosing z_0 such that $f_p(z_0) = mg$ we can take the Laplace transform of Eq. 3 to get $Z(s) = G_{plant}(s)I(s)$ where $Z(s)$ and $I(s)$ are $\mathcal{L}\{z(t)\}$ and $\mathcal{L}\{i(t)\}$, respectively. Therefore, the transfer function of the plant is

$$G_{plant}(s) = \frac{k_i}{m\,s^2 - k_z}\,. \tag{4}$$

The values of the parameters k_i and k_z are $4.7\ \mathrm{N/A}$ and $1.6 \times 10^3\ \mathrm{N/m}$, respectively. Both values were determine through FEM simulations and experiment which will be discussed in more detail in a future publication.

The motion of the LMA changes the separation distance between the LMA and the UMA; this changes the magnetic field between them. A hall sensor, placed between the two magnets, is used to monitor the changing magnetic field. The block dB/Dz represents the conversion between the changes in separation to the change in the magnetic field as measured at the position of the hall sensor and has a value of $21.16\ \mathrm{T/m}$. Now, it is important to recognize that there is another contributing factor to the magnetic field change; namely the magnetic field generated by the electromagnetic coil, denoted as dB/di in Fig. 2. It's value is $0.029\ \mathrm{T/A}$. Both values depend on z_0, here 11.5 mm, and the probe position relative to the UMA (~8 mm). These two magnetic field changes are summed to provide the total magnetic field measured at the hall sensor. The hall sensor has a sensitivity of $5\ \mathrm{V/T}$ and provides some low-pass filtering at $5\ \mathrm{kHz}$. Finally, an additional low-pass filter (~300 Hz) is used before the signal is passed to the PID controller.

The PID transfer function for closed-loop control is

$$K(s) = P\left(1 + I\frac{1}{s} + D\,\frac{N}{1 + N/s}\right). \tag{5}$$

Here $P, I,$ and D are the proportional, integral, and derivative gain terms and N is the filtering coefficient. The filtering coefficient helps smooth the derivative term to avoid sudden changes in the response. The closed loop transfer function is then

$$H(s) = \frac{K(s)G_o(s)}{1 + K(s)G_o(s)} \tag{6}$$

where $G_0(s)$ is the open-loop response composed of all the blocks in Fig. 2 except the controller. As will be discussed in **Sec. 3.5** the PID is actually implemented on a digital system so a discrete version of $H(s)$ is employed. However, given that are control loop is run at 100kHz and the frequency response of $\alpha(s)$ is < 100 Hz, we can effectively treat the system as continuous.

3.4 SIMULATION

To test the closed-loop operation and to verify that the PID parameters that provide a stable control loop, we converted the closed-loop system described above into a Simulink model. In this program the known values for the open-loop system

as described in the previous section are entered. The simulation can then be used to determine PID parameters for stable operation. Also, different test functions can be applied to determine how stable the loop is in the presence of noise and other external perturbations.

In Fig. 3 we show results from a test run where we compare the system response of our model (orange, solid lines) to that of the actually POC (blue, dashed lines). Identical PID parameters were used for both systems: P=50, I=1.5, D=0.5, and N=10. We applied a step-wise change at t=0 equivalent to a change in B-Field of 0.001 V and measured the output at the three monitor points in Fig 2: Control Out [V], Z[m], and B-Field [V]. The agreement in both magnitude and temporal response for the B-Field and Controller Out is excellent. The Z response, which was measured independently using an interferometer, shows good agreement as well.

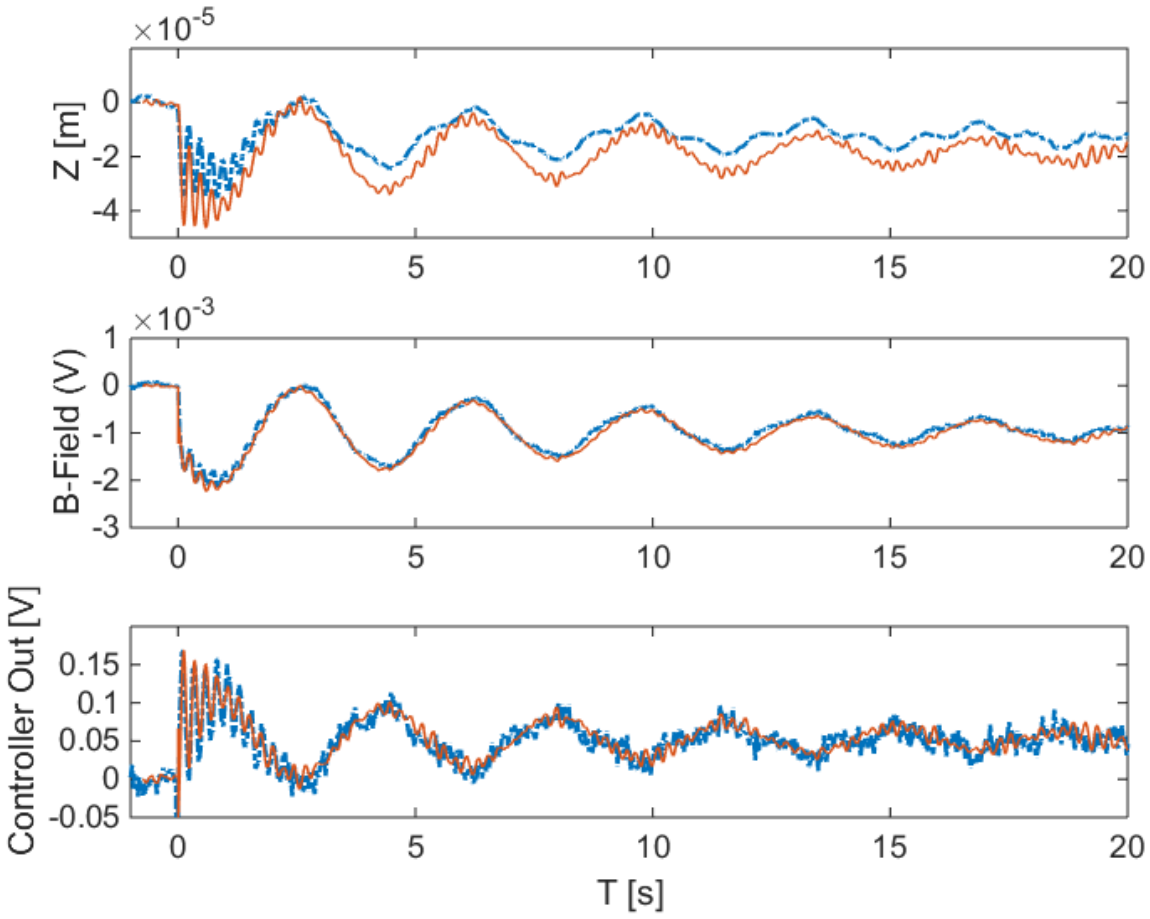

Figure 3: Comparison of response of Simulink model (blue, solid) and real magnetic suspension on POC (blue, dashed) to a step-wise change in the setpoint.

5. IMPLEMENTATION OF CONTROL SYSTEM

In the previous section the model for the magnetic suspension was described and results from an actual magnetic suspension test were compared it. Here we describe how the PID controller was realized in the POC. The implementation of the control loop marks a major upgrade in the magnetic suspension system. The prior realization utilized a standard desktop computer. While suspension was achieved, the level of stability was insufficient to meet our needs. Additionally, standard computer operation like a mouse click would occasionally lead to jumps in the feedback control. The primary

reason for this lies in the time jitter and latency introduce by the operating system. For example, our initial control loop was set to update at a rate of 30 kHz, however while the actual achieved rate peaked at this frequency it showed deviations of several kilohertz, as shown in Fig. 3. Additionally, occasional delays occurred in the loop that lead to peaks at several lower frequencies. All of these problems occurred because the control loop was sharing resources with the non-real time operating system. To completely eliminate this issue we migrated the control loop to a field programmable gate array (FPGA), the red line shows the control loop rate (100 kHz) when running on the FPGA.

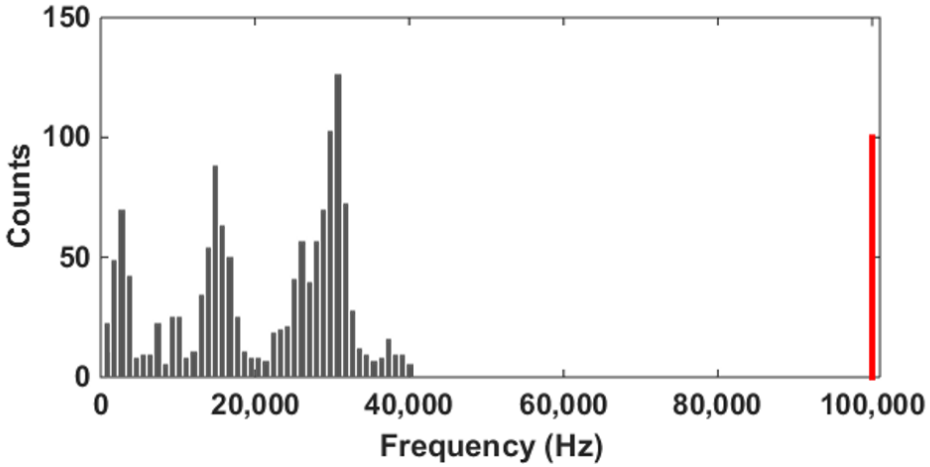

Figure 4: Histogram of frequency distribution of loop-rate for control system implement on desktop computer (gray bars) and FPGA (red line at 100 kHz).

An FPGA allows for programmatically hard-wiring the code through the reconfiguring of gate arrays on an integrated circuit. Because the FPGA uses dedicated hardware to process the control logic, no operating system is involved nor is overhead incurred; this provides real-time determinism. Additionally the logic gates can be set independently, yet synchronized to the same master clock. In this way true parallelism can be realized by allowing multiple control loops to be run simultaneously. Again, since there is no overhead the control loops update rate is fixed and time jitter and latency occur at levels below the inverse of the loop rate. Furthermore, digital filters and real-time monitoring can be added. The FPGA is directly wired to the ADC and DAC and a data stream exists between the FPGA and host computer. This allows real-time monitoring and adjustment of the PID parameters.

The trade-offs when using FPGA include increased complexity in programming, limited physical space on-chip for implementing code, and limited hardware for both ADC and DAC. Since our execution rate is 100 kHz and the master clock is 40 MHz we have plenty of time to accomplish all required tasks within a single cycle of the control loop. While the limited space on the FPGA limits the overall code, we found that we are still able to fit 3 controls loops, multiple filters, and several 'FPGA to Host' transfer lines on a single chip; this far exceeds our base needs. The hardware issue, while currently not a limitation, could be an impediment in the future. The issue lies in the limited resolution of the hardware available for analog-to-digital and digital-to-analog conversion on the FPGA.

5. CONCLUSION

In this paper we described a method for performing direct mass comparison of two masses where one is kept under vacuum and the other in air. Of course the exact environment is of little consequence, but rather the ability to couple the gravitational force acting on the mass in one chamber to the mass comparator in the other is of great utility. This work is primarily focused on dissemination of the standard kilogram in light of the new realization of the kilogram which will occur under vacuum. A further application would include cross checking sorption studies that aim to model the mass added when changing environments.

The primary goal here was to describe the control system and how moving to an FPGA system provides increased stability. In reality it is quite difficult to provide a quantitative result that clearly identifies that the FPGA provides the increased stability that we infer it does. In fact, the best evidence of its benefit comes from direct interaction with the system. Before

implementing the FPGA, manually positioning the suspended mass at a point where stable suspension could occur was difficult. Fluctuations induced by imprecise positioning of the LMA and unsteadiness of the operator's hands when placing the LMA into the proper position for magnet suspension induced large field changes to which, when coupled with the non-deterministic nature of the non-FPGA control loop, could quickly lead to instability. Such instability has been effectively eliminated by the new FPGA based control system.

6. REFERENCES

D. B. Newell," A more fundamental International System of Units," Physics Today **67**, 7 (2014).